

# Deformation of Nuclei Close to the Two-Neutron Drip Line in Mg Region

J. Terasaki, H. Flocard

Division de Physique Théorique\* Institut de Physique Nucléaire,  
91406 Orsay Cedex, France

P.-H. Heenen<sup>†</sup>

Service de Physique Nucléaire Théorique,  
U.L.B.-C.P.229, B-1050 Brussels, Belgium

P. Bonche

SPhT <sup>‡</sup>-CEA Saclay, 91191 Gif sur Yvette Cedex, France

February 26, 2019

## Abstract

We perform the Hartree-Fock-Bogoliubov (HFB) calculations for ground states of even Mg isotopes using the Skyrme force and a density-dependent zero-range pairing force. The HFB equation is solved in a three-dimensional cartesian mesh, and a convergence of deformation is carefully examined with respect to a cut-off radius for a check of the calculations. We discuss systematics of the two-neutron separation energy, deformation and root-mean-square radius. We have found that  $^{36,38,40}\text{Mg}$  have appreciable static deformation, where  $^{40}\text{Mg}$  is a two-neutron drip-line nucleus in our calculation, and the deformations of the neutron and proton are different in these three nuclei. The deformation property is analyzed on the basis of the single-particle diagram. It is shown that  $N = 28$  is not a closed shell in Mg as well as Si.

## 1 Introduction

The existence of deformed drip-line nuclei has been recently questionned [1] on the basis of a detailed analysis of the available data. Tanihata et al. argued that with few exceptions, the last bound isotopes of a chain could be related to a sub-shell closure in a spherical shell model. The number of cases entering such an analysis is however limited since the neutron drip line is known only up to  $Z=9$ . To confront the justification of this analysis by means of fully microscopic calculations is not an easy task: most studies of drip-line nuclei have been

---

\*Unité de recherches des Universités Paris XI et Paris VI associée au CNRS.

<sup>†</sup>Directeur de Recherches FNRS.

<sup>‡</sup>Laboratoire de la DSM

restricted to spherical shapes [2, 3, 4, 5, 6]. On their basis, it has been suggested that the single particle gaps associated with magic numbers significantly decrease near the drip lines [2]. On the other hand, two recent studies of deformation in the Mg[7] and Si-Ca[8] regions have been performed with pairing correlations limited to the constant gap-BCS approximation. Sizable deformations were found for some drip line nuclei. However, no definite conclusions can be drawn from these studies as the BCS approximation breaks down when bound and unbound single-particle states interact via the pairing[9].

In a recent publication[10], we have presented a method based on the solution of the Hartree-Fock-Bogoliubov (HFB) equations on a 3-dimensional cartesian mesh. It describes consistently both the pairing correlations and the asymptotic behaviour of wave functions of weakly bound systems. The effective interaction is split in two parts: a Skyrme force to describe the mean-field (particle-hole channel) and a density-dependent zero-range force for the pairing correlations (particle-particle channel). The tests on the even Ni isotopes have shown that this method accounts correctly for the interactions between bound and continuum single-particle states. The fact that all these isotopes are spherical made the analysis of our results easier because of the degeneracy of individual wave functions. Nevertheless the scope of the method presented in ref.[10] is broader since all single particle states were calculated in a three-dimensional geometry as for a triaxially deformed nucleus.

In this work, we have chosen the Mg isotopes as large deformations for the heaviest isotopes have been predicted on the basis of the BCS approximation. Together with neighboring isotopic chains, these nuclei have been extensively studied experimentally. Many of the experimental works pay great attention to deformation of  $N = 20$  nuclei in  $A = 30$  mass region. Isotope shifts of some Na nuclei were measured by Huber et al. [11] and Touchard et al. [12]. Huber et al insist that  $^{31}\text{Na}$  is deformed, however Touchard et al concluded that no evidence of sudden onset of deformation at  $N = 20$  was found in Na from their isotope shift. Détraz et al [13] argue that  $^{32}\text{Mg}$  is deformed on the basis of the systematics of energies of the first  $2^+$  states which they have measured through the  $\beta$ -decays and the measured masses of  $^{31,32}\text{Mg}$  [14]. Gillibert et al. [15] measured masses including  $^{30-32}\text{Na}$  and  $^{31-33}\text{Mg}$  and observed a flattening of a curve of the two-neutron separation energy,  $S_{2n}$ , at  $N = 20$ , while Vieira et al. [16] have obtained no irregularity in the  $S_{2n}$  curve in  $^{30-32}\text{Mg}$  and  $^{32-34}\text{Al}$ . Motobayashi et al. [17] have measured large  $B(E2)$  value from the first  $2^+$  state to the ground state in  $^{32}\text{Mg}$ . This indicates strongly the deformation of  $^{32}\text{Mg}$ . For  $^{33}\text{Al}$  Woods et al. [18] also concluded that the nucleus had a good shell closure based on their measurement of the mass. Woods et al. [19] concluded that deformation of  $^{34}\text{Si}$  was unlikely from a comparison of their measured masses with a result of the shell-model calculation. This conclusion is consistent with the mass measurement of  $^{33,34}\text{Si}$  made by Fifield et al. [20]. Smith et al. [21] measured the mass of  $^{35}\text{Si}$  and argue that the nucleus is not deformed from the systematics of  $S_{2n}$ . The one-proton drip line, or nuclei very close to it, was explored by Langevin et al. [22]. They have observed  $^{23}\text{Si}$ ,  $^{27}\text{S}$ ,  $^{31}\text{Ar}$  and  $^{35}\text{Ca}$ . Schwalm et al. [23] measured static quadrupole moments of the first  $2^+$  states of  $^{20,22}\text{Ne}$ ,  $^{24,26}\text{Mg}$  and  $^{28}\text{Si}$ . Charge root-mean-square radii of  $^{24-26}\text{Mg}$  were reported by Lees et al. [24]. Recently Suzuki et al. [25] reported matter root-mean-square radii of many Na and Mg isotopes from the interaction cross sections.

Several shell-model calculations [26, 27, 28, 29, 30] also have been performed in Mg isotopes, and it was clarified that the inclusion of the f shell was crucial for reproducing properties of  $^{32}\text{Mg}$ . Their studies support the deformation of  $^{32}\text{Mg}$ . On the other hand, as compared to these

works, systematic mean-filed calculations in Mg isotopes have been scarce until very recently. This paper presents an investigation of the deformation properties of the even Mg isotopes from the proton to the neutron drip line. At the neutron drip line, we have also studied the neutron rich Ne and Si isotopes.

## 2 Strength of the pairing interaction

In our method, different parametrizations for the interaction are chosen for the mean-field and the pairing channels. For the particle-hole channel, a Skyrme force is used. We have employed two parameter sets. The first one is SIII [31], which has been extensively used to study deformation properties with much successes. The second one, Sly4 [32], has been recently adjusted with a special attention to the properties of infinite nuclear and neutron matters. It is expected to provide a more realistic isospin dependence than previous forces. Such a choice of two different parametrizations of the effective force allows a test of their reliability away from the stability region where they have been adjusted.

For the pairing channel, a density-dependent zero-range force is used:

$$V_P(\mathbf{r}_1, \mathbf{r}_2) = V_0(1 - P_\sigma)(1 - \frac{\rho(\mathbf{r}_1)}{\rho_c}) \delta(\mathbf{r}_1 - \mathbf{r}_2) \quad (1)$$

where  $P_\sigma$  is the spin exchange operator and  $\rho(\mathbf{r})$  the total nuclear density.  $V_0$  is the strength of the force, chosen to be the same for neutrons and protons, and  $\rho_c$  is a constant which determines the density dependence. In this work we fix  $\rho_c = 0.16\text{fm}^{-3}$ , which is close to the nuclear saturation density. This force is strongly attractive around the nuclear surface, a property which has been discussed in [4].

As extensively discussed in our previous paper[10], reliable results for drip line nuclei require that two conditions are met. The dimension of the box in which the HF equations are solved must be large enough to describe correctly the tail of the wave functions. The use of the imaginary time method enables to solve the mean-field equations for a limited number of orbitals; this number must be large enough to ensure a correct description of the continuum wave functions. In this application to Mg isotopes, we have used the values for the box size (15 fm) and for the number of single-particle wave functions explicitly calculated (70 for neutrons and 35 for protons) that were shown sufficient in our Ni calculation. Since this study is devoted to much lighter nuclei, these values are large enough. We also performed selected tests which fully confirmed the conclusions of our previous study. A smooth cut-off of the pairing interaction at an energy of 5 MeV above the fermi level has been introduced following the procedure explained in ref[33].

The Mg isotopes do not constitute a favourable region for an adjustment of the pairing strength  $V_0$ . Pairing correlations are weak in light nuclei making the determination of experimental quasi-particle energies from binding energies not very accurate. Moreover, the variation of these binding energies are affected by the strong dependence of the shape of Mg isotopes on the neutron number, an effect which should not be included in the determination of quasi-particle energies. The value  $V_0 = 1000\text{MeVfm}^3$  for SIII and SLy4 has been found reasonable in previous studies of superdeformation in both the  $A=150$  and  $190$  mass regions. We have therefore chosen to test these values for the Mg isotopes. For this purpose, we have compared the experimental and theoretical values obtained for the two-neutron separation energies  $S_{2n}(N, Z)$ ,

calculated from the difference between the HFB ground state energies of neighbouring even nuclei. An often very good approximation of  $S_{2n}(N, Z)$  is provided by the quantity  $-2\lambda_n$ , where  $\lambda_n$  is the HFB chemical potential. To determine the sensitivity of the results to the value of  $V_0$ , we have also performed a set of calculations with  $V_0=700\text{MeVfm}^3$ . Our results are plotted on Fig. 1 together with the experimental data. The  $S_{2n}$  values are clearly insensitive to  $V_0$ . They are also quite similar for both Skyrme parametrizations. The global trends of the experimental data are satisfactorily reproduced. The shell effect at  $N=20$  disappears experimentally in  $^{32}\text{Mg}$ . This is consistent with the large scale shell model calculations of ref [30]. In this respect, the results obtained with SIII are more consistent with the experimental data than with SLy4, although in both cases the shell effect is weak. The problems posed by the description of  $^{32}\text{Mg}$  will be discussed in a forthcoming publication.

In the following, we shall use  $V_0 = 1000\text{MeVfm}^3$  for both SIII and SLy4. These strengths give a reasonable agreement with the experimental data for the  $S_{2n}$  values. We have also checked that they lead to qp energies in  $^{24}\text{Mg}$  close to the experimental ones. More importantly, the use of the same values as in our studies of superdeformation seems to indicate that a unique parametrization of a density-dependent zero-range pairing interaction may be used over the whole nuclear chart. With these pairing strengths, pairing correlations vanish for protons in  $^{36-40}\text{Mg}$  and for neutrons in  $^{20}\text{Mg}$  and  $^{26}\text{Mg}$ .

On Fig. 2, we compare the experimental data for  $S_{2n}$  as a function of  $A$  [34] to the prediction of different models. In our calculations the two-neutron drip line is located between  $^{40}\text{Mg}$  and  $^{42}\text{Mg}$  for both SIII and SLy4. The lightest Mg isotope predicted to be bound against two protons decay is  $^{20}\text{Mg}$ . Its two-proton separation energy is equal with SIII to 3.31 MeV, to be compared with 2.33 MeV experimentally. The other theoretical approaches have been specifically designed to reproduce nuclear masses and lead to a better agreement with the experimental data than our calculation. However above the experimentally known region, their predictions for  $S_{2n}$  show irregularities which are probably spurious. Nevertheless, the trends obtained with the relativistic mean field (RMF) theory [35, 7] and the finite-range droplet model (FRDM) [36], are similar except for  $^{20,22}\text{Mg}$  and for a slight increase of  $S_{2n}$  from  $^{38}\text{Mg}$  to  $^{40}\text{Mg}$  in the RMF by Hirata et al. and FRDM. Thus it seems that the location of the two-neutron drip line does not significantly depend on a theoretical approach, as far as those three typical methods are concerned. Hereafter we shall discuss the results obtained with SIII unless otherwise specified.

### 3 Deformation properties of the Mg isotopes

Fig. 3 shows the variation of the energy of all isotopes calculated in Mg chain, as a function of their axial quadrupole moment. The energy curve of  $^{20}\text{Mg}$  is the most rigid. Its spherical minimum is due to the magic neutron number  $N=8$ . Marked prolate deformations are obtained from  $^{36}\text{Mg}$  to  $^{40}\text{Mg}$ . In these three cases, a very shallow oblate minimum appears at an excitation energy of 1.0 MeV. In particular, we find that the neutron shell effect at  $N = 28$  is suppressed at the drip line. An interesting point is that the introduction of deformations does not modify strongly the dependence on the neutron number of the mean-field value obtained for  $S_{2n}$ . Deformations only bring a gain of energy of 1 MeV at  $^{36}\text{Mg}$  where deformation sets in, but the values for the heavier isotopes are qualitatively not affected.

Since  $^{40}\text{Mg}$  is bound by less than 2.0 MeV, we have investigated whether the large quadrupole moment of the ground state is not due to a neutron halo surrounding the nucleus which could be

not properly described by our calculation. For this purpose, we have first checked the stability of the number of neutrons outside a 15 fm diameter sphere as a function of the box size  $R$ :

$$N_{\text{out}} = \int_{r \geq 15\text{fm}} \rho_n(\mathbf{r}) d^3\mathbf{r}, \quad (2)$$

where  $\rho_n(\mathbf{r})$  is the neutron density. We have obtained  $N_{\text{out}} = 0.430 \times 10^{-2}$  and  $0.683 \times 10^{-2}$  for box sizes  $R = 16$  and  $18$  fm, respectively. These quite small and nearly constant values indicate the absence of a halo and that the quadrupole moment is due to neutrons bound into the nucleus.

To determine the location of the nucleons responsible for the deformation, we have introduced a cutoff variable  $r_{\text{in}}$  and calculated a deformation parameter  $\beta(r_{\text{in}})$  by including the contribution to the square radius and to the quadrupole moment of the nucleons located below the radius  $r_{\text{in}}$ :

$$Q(r_{\text{in}}) = \int_{r \leq r_{\text{in}}} Q(\mathbf{r}) \rho(\mathbf{r}) d^3\mathbf{r}, \quad (3)$$

$$\overline{r^2}(r_{\text{in}}) = \int_{r \leq r_{\text{in}}} r^2 \rho(\mathbf{r}) d^3\mathbf{r}, \quad (4)$$

$$\beta(r_{\text{in}}) = (\pi/5)^{1/2} \frac{Q(r_{\text{in}})}{\overline{r^2}(r_{\text{in}})} \quad (5)$$

respectively, where  $\rho(\mathbf{r})$  was taken from the result of  $R = 18$  fm. These quantities are defined separately for neutrons and protons. Fig. 4 shows  $\beta(r_{\text{in}})$  for neutrons and protons in  $^{40}\text{Mg}$ . One sees that the asymptotic value of the deformation is reached when  $r_{\text{in}}$  is larger than  $5/3$  of the root-mean-square radius of the nucleus, 3.6 fm. This demonstrates that the observed differences in  $\beta$  are core effects and do not result from a decoupling of neutrons and protons.

An interesting feature apparent for  $^{40}\text{Mg}$  on Fig. 4 is the significant difference in deformation between the neutrons and the protons. The neutron and proton parameters  $\beta$  along with a few experimental data and the total quadrupole moments are plotted for all the Mg isotopes in Fig. 5.  $\beta$  and the quadrupole moments of secondary minima are also indicated when present. For light isotopes, neutron and proton deformations are similar. For  $^{24}\text{Mg}$ , the presence of the deformed shell effects at 12 for both neutrons and protons (see Fig. 6) leads to the most deformed nucleus of the isotopic chain. At  $N=20$ , the shell closure for neutrons is strong enough to compensate the effect of the proton deformed shell closure. As soon as the  $f_{7/2}$  shell starts to be filled, the proton effect gains, leading to strong deformations in  $^{36-40}\text{Mg}$ . One indeed recovers in these nuclei a similar proton deformation as in  $^{24}\text{Mg}$ .

For the experimental data of  $^{24,26}\text{Mg}$  more accurate measurements are desired for a comparison with our calculated result.  $^{26}\text{Mg}$  is a nucleus having the shape coexistence and favors slightly the oblate state in our calculation.  $^{32}\text{Mg}$  is clearly a problem. As far as we know, there is no mean-field calculation which can reproduce  $\beta \simeq 0.5$  of  $^{32}\text{Mg}$  with a reasonable effective interaction.  $^{32}\text{Mg}$  is the only isotope for which the deformation energy curve shows a structure at a deformation larger than the absolute minimum of the spherical shape. It indicates that correlations beyond the mean field approximation are probably required to explain the experimental  $\beta$  and the low energy  $2^+$  state with a large BE2 value observed experimentally [17]. Fig. 6 shows calculated root-mean-square radii and experimental data. It is seen that our calculation reproduces the measured data quite well except for  $^{24}\text{Mg}$ . An influence of the sudden

onset of the prolate deformation in  $^{36}\text{Mg}$  appears in a small irregularity of the calculated curves. The irregularity is, however, so small that if one wants to confirm an appreciable change in deformation on the basis of radii, much accurate measurements would be required.

The single particle level energies in the canonical basis are shown on Fig. 7 for  $^{40}\text{Mg}$ ; except mainly for shifts in energies, the same plot is valid for all the isotopes. The fermi level for the neutrons in  $^{40}\text{Mg}$  is close to 0, with a quadrupole moment for the ground state of 1.85 b. The neutron deformation is smaller in this nucleus because the larger density of levels near the fermi surface leads through pairing correlations to the population of orbitals with a less deformation driving character than the  $\pi d_{5/2}$  orbital. These different deformations are only possible because the numbers of neutrons is much larger than the number of protons. Otherwise the large overlap between the neutron and proton densities induced by the neutron-proton interaction would suppress the differences in deformations.

Qualitatively similar results have been obtained in the RMF calculation of Ren et al.[7]. Both  $^{20}\text{Mg}$  and  $^{32}\text{Mg}$  have been found spherical by these authors and  $^{36-40}\text{Mg}$  very deformed. However, the quadrupole moments of deformed isotopes are significantly larger in the RMF calculation. This may be related to the BCS apporximation with a constant gap used by Ren et al.

The  $N = 28$  neutron gap is not apparent neither in the  $S_{2n}$  nor in the evolution of the radii. On Fig. 7, one can see that the value of this gap is of 3 MeV in  $^{40}\text{Mg}$ , to be compared to the 5 MeV of  $^{48}\text{Ca}$  calculated in ref. [31]. This quenching of the  $N = 28$  gap is sufficient to allow the deformed proton gap at  $Z = 12$  to take over. Similar results have been obtained in the study of Si and S isotopes [8]

Fig. 8 shows the potential energy curves of the  $N = 28$  Si isotope  $^{42}\text{Si}$  and of the two drip line nuclei  $^{34}\text{Ne}$  and  $^{46}\text{Si}$ . The energy curves of these three isotopes display a soft dependence on the quadrupole moment. This is an indication that dynamical collective effects built on the quadrupole mode are important. One notes also that there is no sign of a spherical shell effect at  $N = 28$  for  $^{42}\text{Si}$  as was the case already in  $^{40}\text{Mg}$  . Similar results have been obtained by Werner et al[8] with the HF+BCS approximation.

## 4 Conclusion

In this paper, we have reported the first calculation of drip line nuclei based on a mean field approach where quadrupole deformations are included and pairing correlations are correctly treated. We have shown that deformation effects cannot be neglegted to describe the neutron rich Mg isotopes.

One of the main conclusions of this work is the disappearance of the  $N=28$  shell closure close to the drip line. There is indeed in Mg isotopes a competition between the deformed shell effect at  $Z=12$  and the  $N=28$  spherical shell closure. The population of neutron deformation driving orbits thanks to pairing correlations favours the occurence of deformation in the last bound Mg isotopes. An interesting consequence of the large excess of neutrons with respect to the protons is the appearance of significantly different neutron and proton deformations. If confirmed experimentally, this feature may lead to new isovector excitation modes in isotopes close to the drip lines.

Our calculation does not confirm the conjecture of Tanihata et al that all drip lines are spherical. The small number of drip line nuclei known experimentally may explain the probable

failure of this conjecture. Our results stress once more the importance of a better knowledge of the neutron drip line.

## References

- [1] I. Tanihata, D. Hirata and H. Toki, Nucl. Phys. **A583** (1995) 769
- [2] J. Dobaczewski, I. Hamamoto, W. Nazarewicz and A. Sheikh, Phys. Rev. Lett. **72** (1994) 981
- [3] J. Dobaczewski, W. Nazarewicz and T. R. Werner, Z. Phys. A **354** (1996) 27
- [4] J. Dobaczewski, W. Nazarewicz, T. R. Werner, J. F. Berger, C. R. Chinn and J. Decharge, Phys. Rev C **53** (1996) 2809
- [5] D. Hirata, H. Toki, T. Watabe, I. Tanihata and B. V. Carlson, Phys. Rev. C **44** (1991) 1467
- [6] R. Smolańczuk and J. Dobaczewski, Phys. Rev. C **48** (1993) R2166
- [7] Z. Ren, Z. Y. Zhu, Y. H. Cai and G. Xu, Phys. Lett. B **380** (1996) 241
- [8] T.R. Werner, J.A. Sheikh, M. Misu, W. Nazarewicz, J. Rikovska, K. Heeger, A.S. Umar and M.R. Strayer, Nucl. Phys. **A597** (1996) 327
- [9] J. Dobaczewski, H. Flocard and J. Treiner, Nucl. Phys. **A422** (1984) 103
- [10] J. Terasaki, P.-H. Heenen, H. Flocard and P. Bonche, Nucl. Phys. A **600** (1996) 371
- [11] G. Huber et al. Phys. Rev. C **18** (1978) 2342
- [12] F. Touchard et al. Phys. Rev. C **25** (1982) 2756
- [13] C. Détraz, et al. Phys. Rev. C **19** (1979) 164
- [14] C. Détraz et al. Nucl. Phys. A **394** (1983) 378
- [15] A. Gillibert et al. Phys. Lett. B **192** (1987) 39
- [16] D. J. Vieira et al. Phys. Rev. Lett. **57** (1986) 3253
- [17] T. Motobayashi et al., Phys. Lett. B **346** (1995) 9
- [18] D. J. Woods et al. Phys. Lett. B **182** (1986) 297
- [19] P. J. Woods et al. Z. Phys. A **321** (1985) 119
- [20] L. K. Fifield et al. Nucl. Phys. A **440** (1985) 531
- [21] R. J. Smith et al. Z. Phys. A **324** (1986) 283
- [22] M. Langevin et al. Nucl. Phys. A **455** (1986) 149

- [23] D. Schwalm et al., Nucl. Phys. A **192** (1972) 449
- [24] E. W. Lees et al., J. Phys. G **2** (1976) 105
- [25] T. Suzuki et al. private communication
- [26] B. H. Wildenthal and W. Chung, Phys. Rev. C **22** (1980) 2260
- [27] A. Watt, R. P. Singhal, M. H. Storm and R. R. Whitehead, J. Phys. G **7** (1981) L145
- [28] A. Poves and J. Retamosa, P. L. B **184** (1987) 311
- [29] E. K. Warburton, J. A. Becker and B. A. Brown, Phys. Rev. C **41** (1990) 1147
- [30] N. Fukunishi, T. Otsuka and T. Sebe, Phys. Lett. B **296** (1992) 279
- [31] M. Beiner, H. Flocard, N. Van Giai and P. Quentin, Nucl. Phys. A **238** (1975) 29
- [32] E. Chabanat, P. Bonche, P. Haensel and R. Schaeffer, Phys. Script. **T56** (1995) 231, and private communication.
- [33] P. Bonche, H. Flocard, P.-H. Heenen, S.J. Krieger and M.S. Weiss, Nucl. Phys. A **443** (1985) 39
- [34] G. Audi and A. H. Wapstra, Nucl. Phys. A **565** (1993) 66
- [35] D. Hirata, private communication
- [36] P. Möller, J. R. Nix, W. D. Myers and W. J. Swiatecki, Atom. Data and Nucl. Data Tables **59** (1995) 185

## Figure Captions

Fig. 1 Calculated and experimental  $S_{2n}$  for  $A = 22\text{--}34$ . Two strengths of the pairing force,  $V_0 = 1000$  and  $700 \text{ MeV fm}^3$ , were used. a) The parameter set SIII for the Skyrme force was used. b) The parameter set SLy4 was used.

Fig. 2 Calculated and experimental  $S_{2n}$ . The calculated points are extended up to the two-neutron drip line. In our calculation the parameter set SIII is used. Results of a RMF and FRDM calculations were taken from refs. [7] and [34], respectively.

Fig. 3 Potential energy curves calculated for even  $^{20\text{--}40}\text{Mg}$  isotopes by using SIII as functions of the total quadrupole moment with the axial symmetry retained. The origin of the energy is always taken to be the minimum of the curves.

Fig. 4  $\beta$  calculated with the cut-off radius  $r_{in}$  for proton and neutron of  $^{40}\text{Mg}$ . See eqs. (3)–(5).

Fig. 5 Calculated and experimental  $\beta$  (upper panel) and calculated total quadrupole moments (lower panel) versus  $A$  in the Mg isotopes. The symbols connected by lines are results for the calculated ground states, and the isolated symbols of the calculation correspond to the second minimum found in the potential energy curves. The experimental  $\beta$  of  $^{24,26}\text{Mg}$  were obtained from refs. [23] and [24], and that of  $^{32}\text{Mg}$  was taken from [17].

Fig. 6 Calculated and experimental rms radii versus  $A$ . The symbols with lines attached are calculated results. The black stars are matter rms radii of [25], and white stars are charge rms radii taken from [24].

Fig. 7 Single-particle energy diagrams of  $^{40}\text{Mg}$  as functions of the total quadrupole moment. These are diagonal elements of the HF Hamiltonian in the canonical base. The upper (lower) is of neutron (proton).

Fig. 8 Potential energy curves of  $^{34}\text{Ne}$  and  $^{42,46}\text{Si}$ . Meanings of  $E$  and  $Q$  are the same as those of Fig. 3.  $^{34}\text{Ne}$  and  $^{46}\text{Si}$  are two-neutron drip-line nuclei in the two isotopic chains.

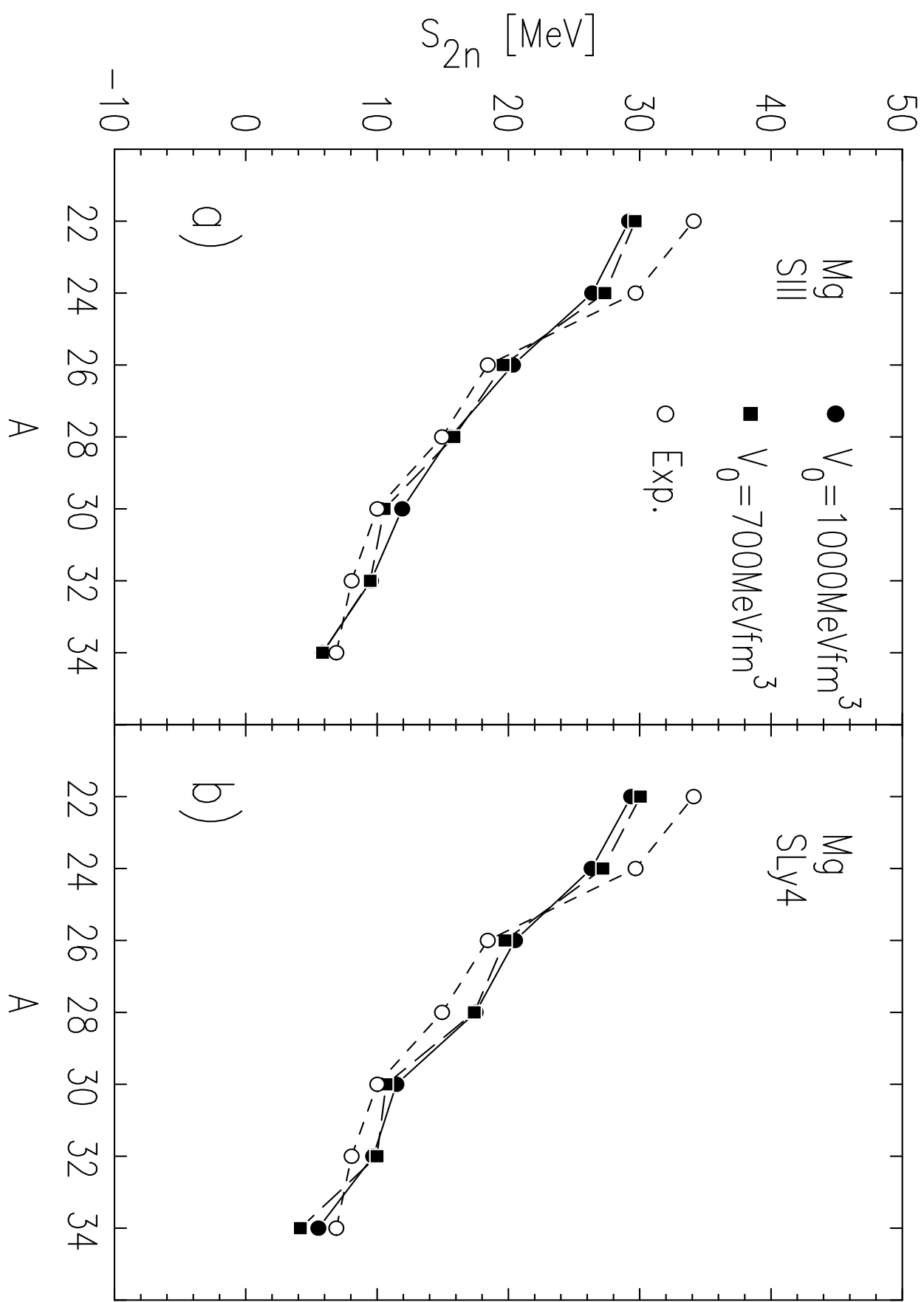


Fig. 1

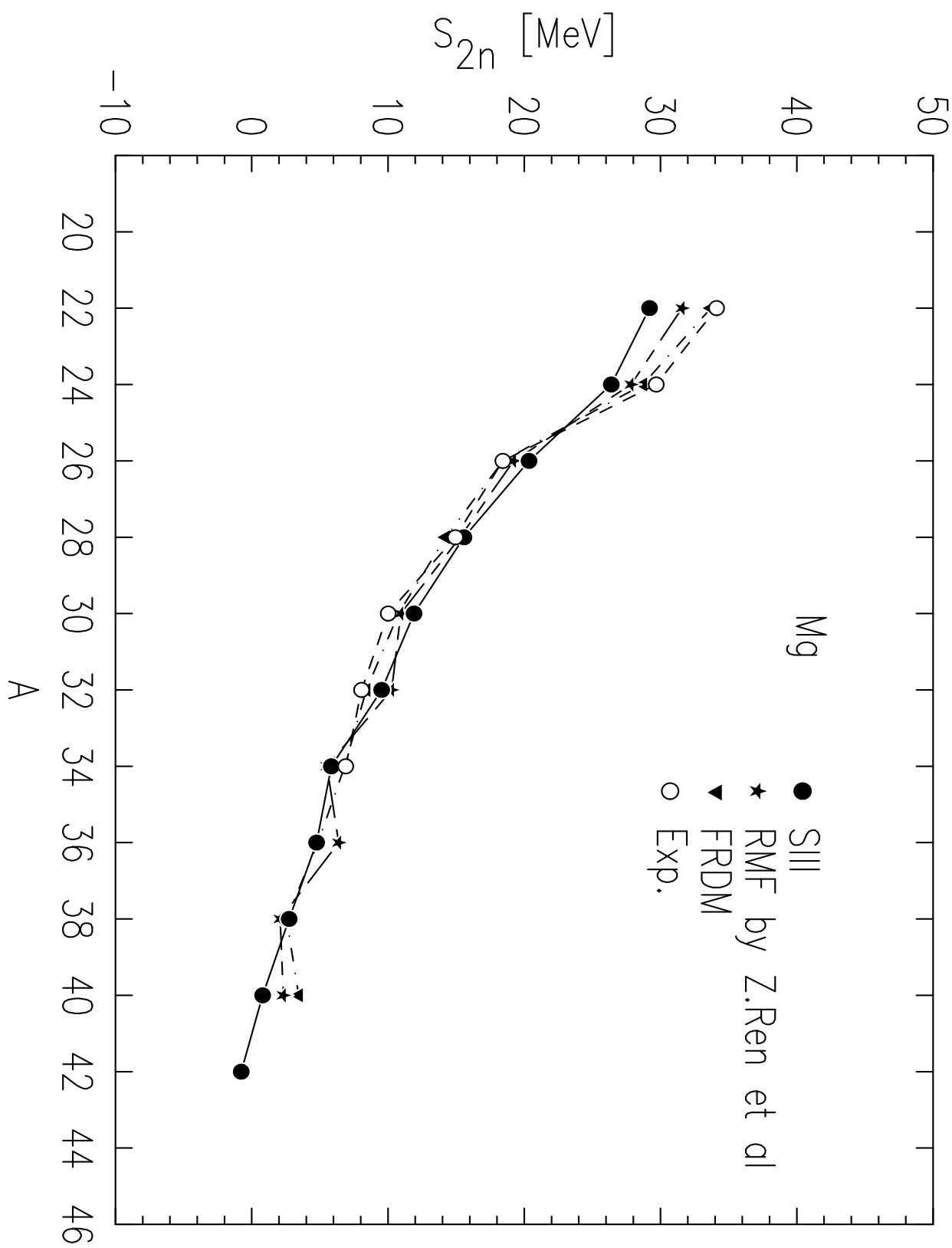


Fig.2

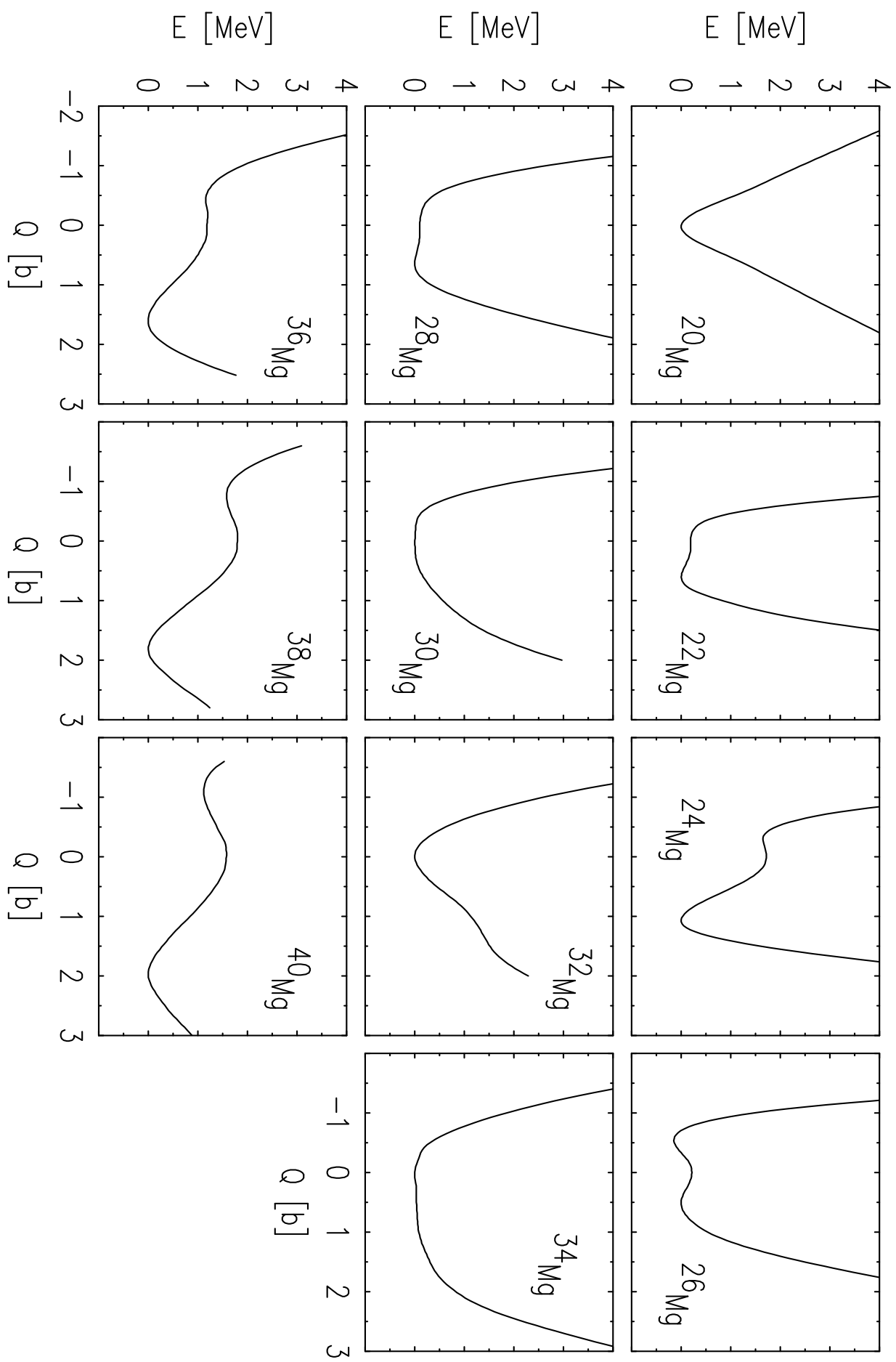


Fig.3

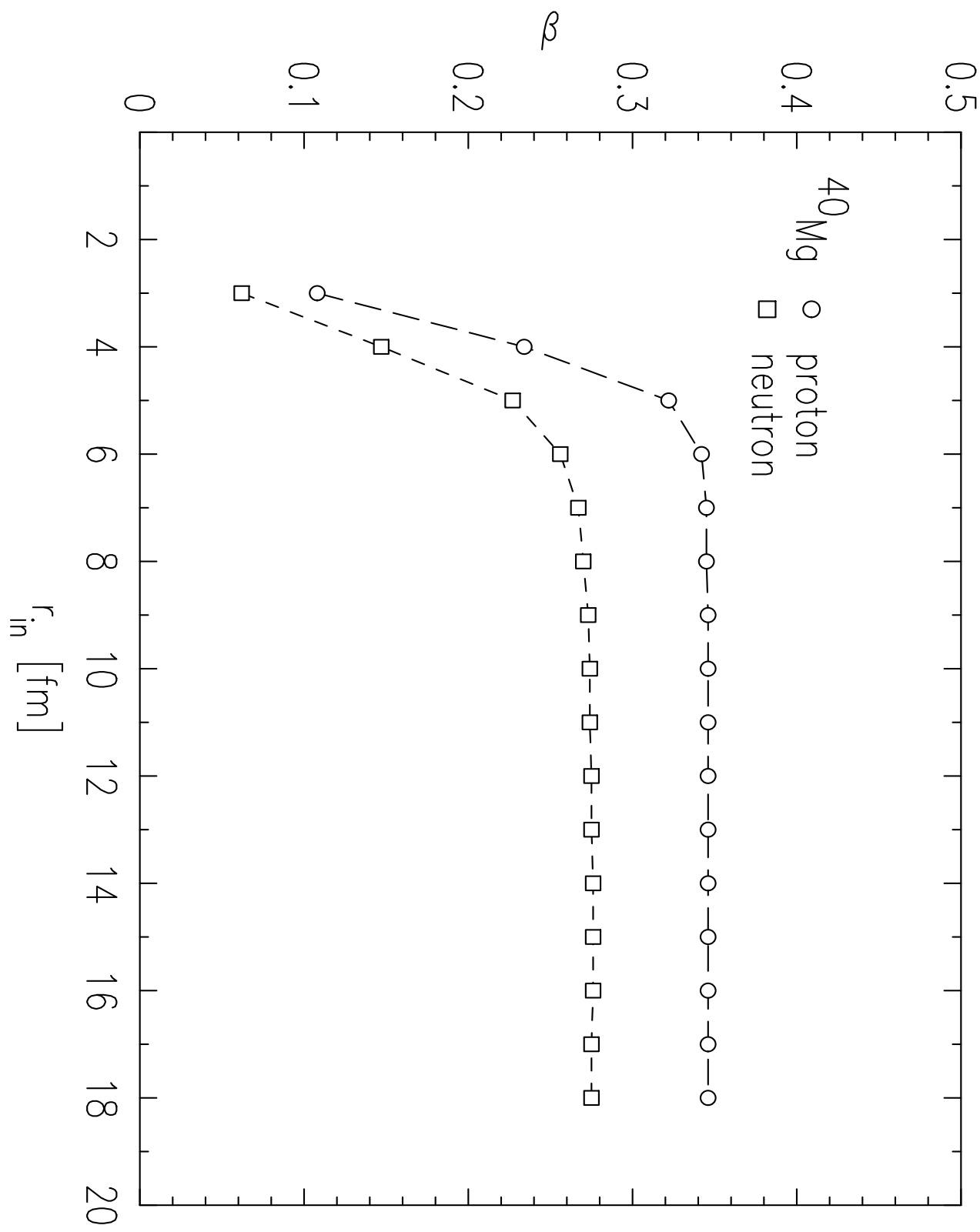


Fig.4

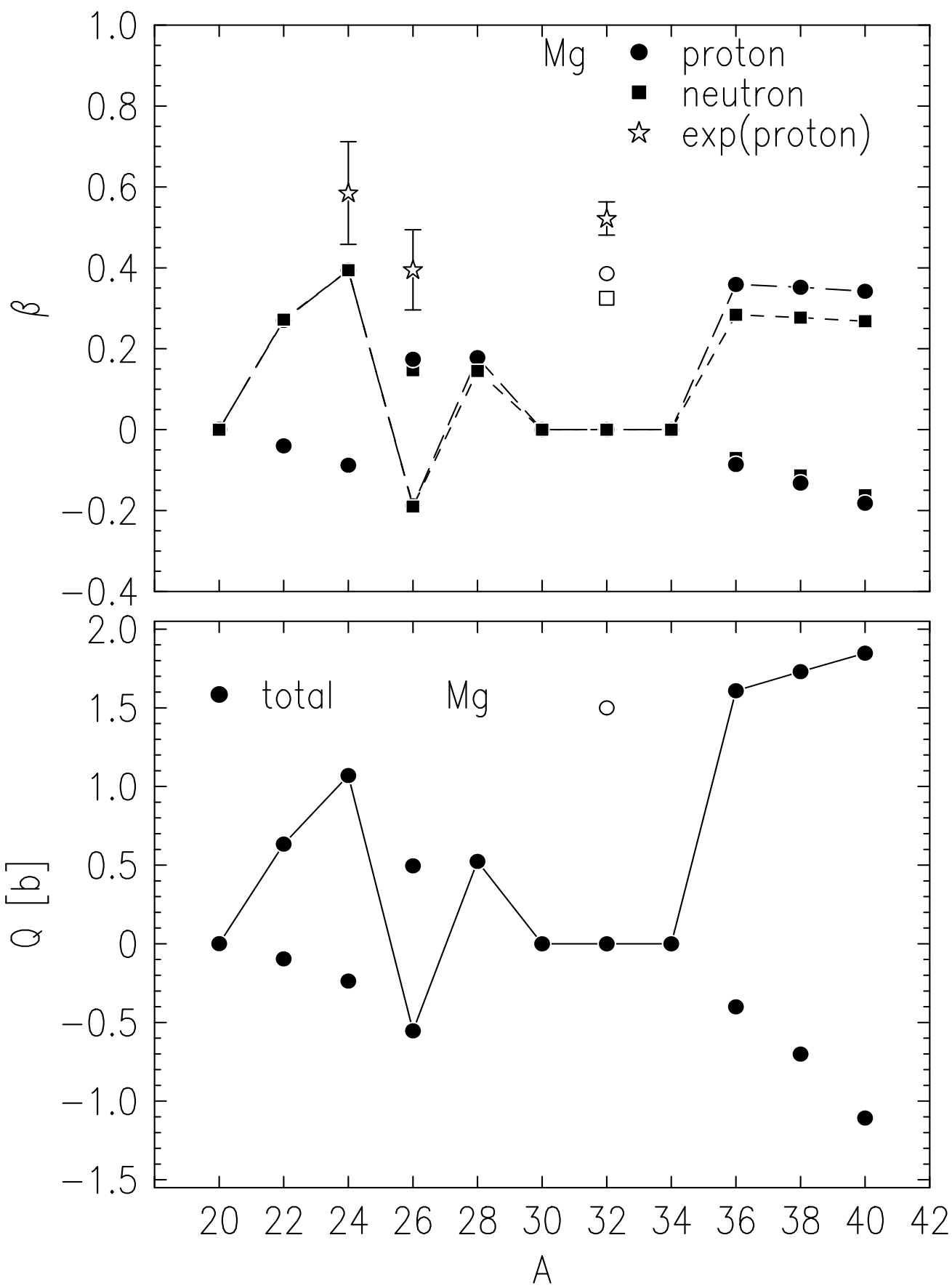


Fig.5

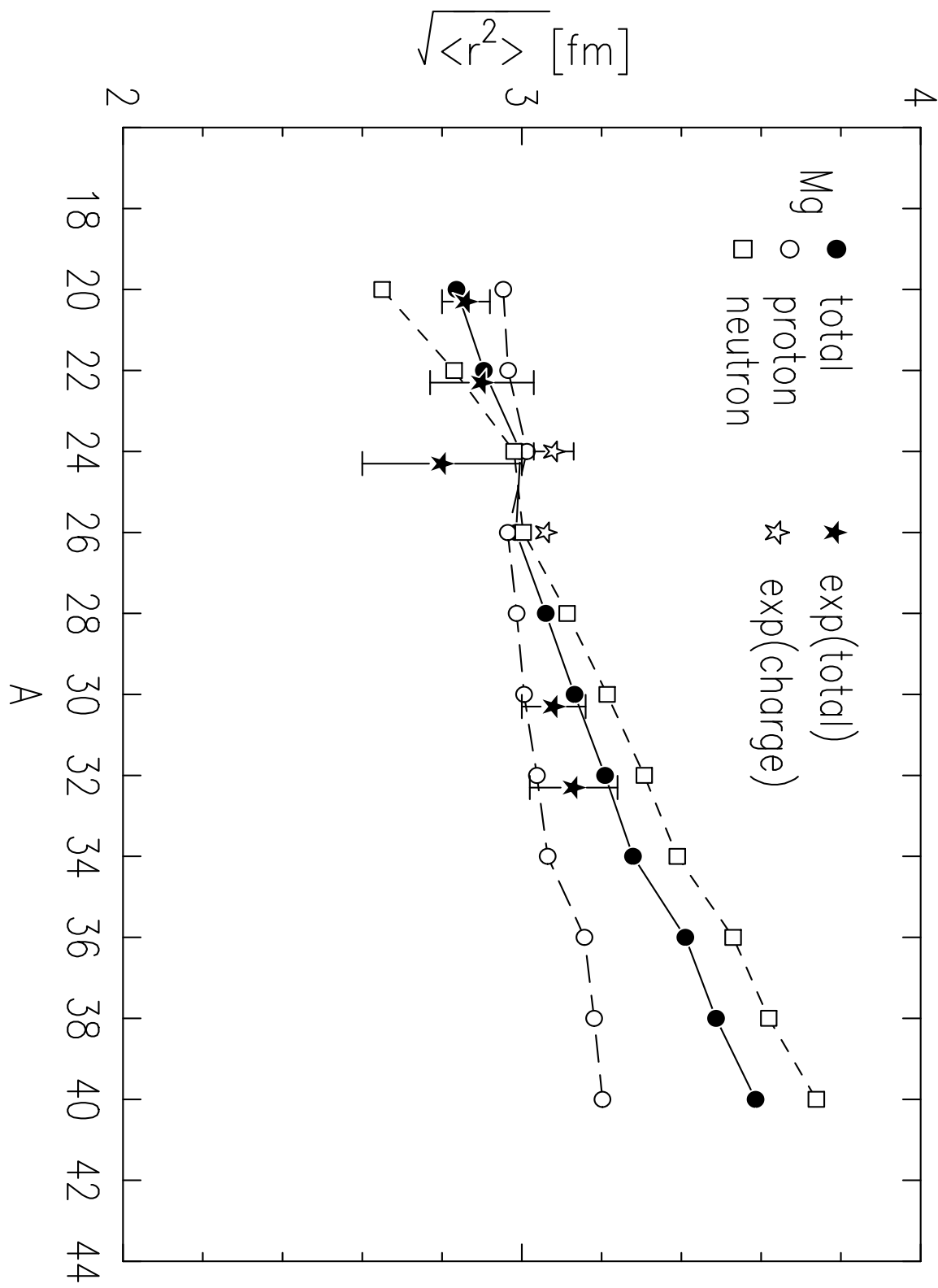


Fig.6

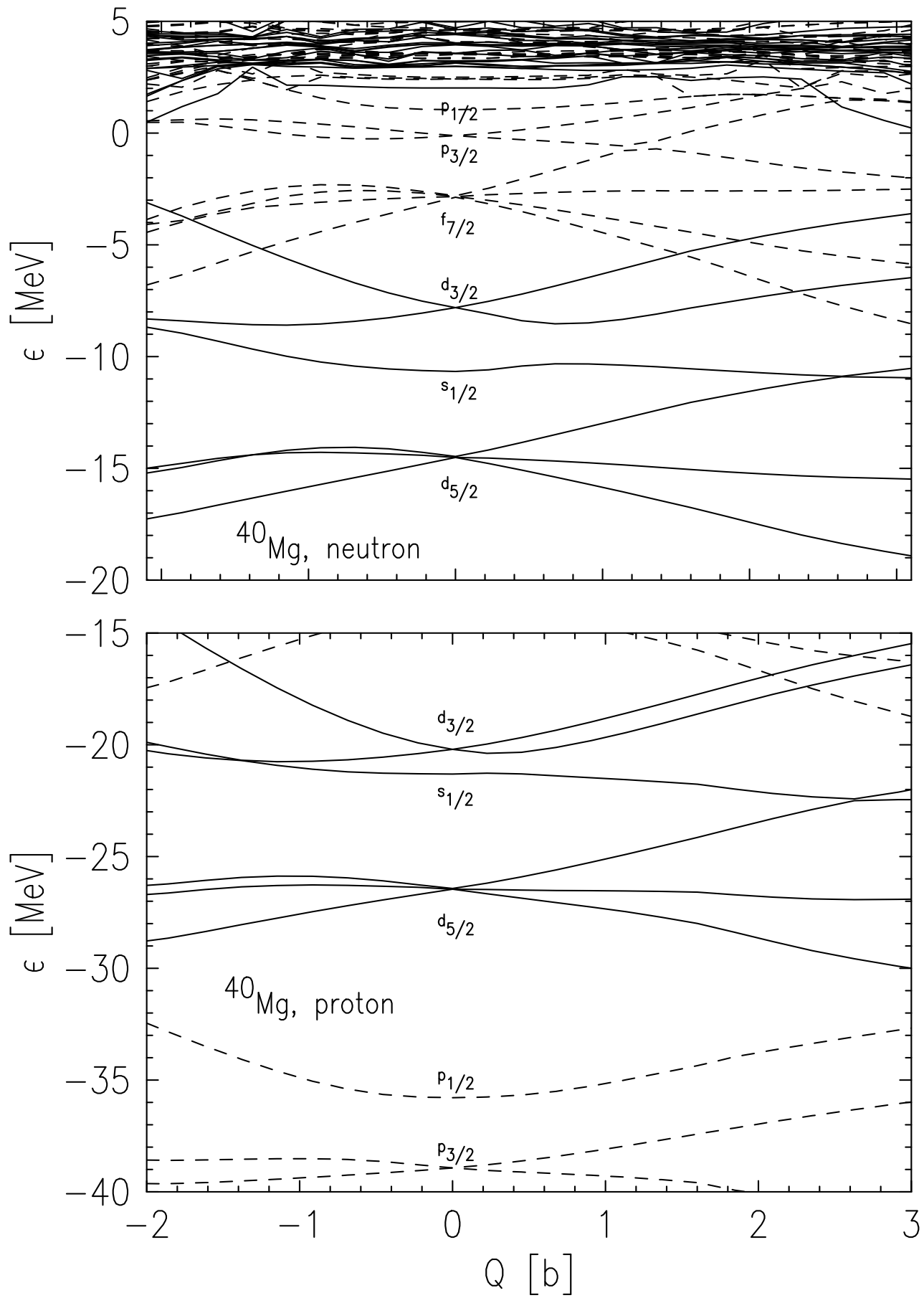


Fig.7

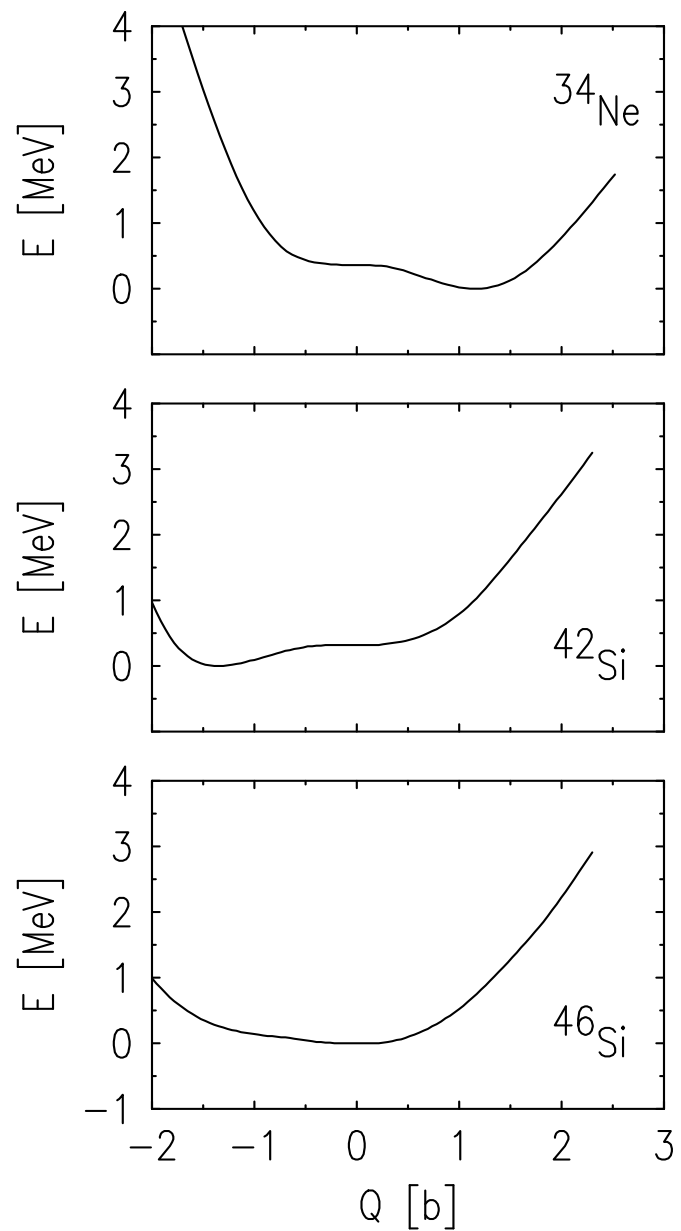


Fig.8